2002

Pressure Drop and Heat Transfer Of Microfinned Microchannels

C. A. Monroe
University of Illinois at Urbana-Champaign

T. A. Newell
University of Illinois at Urbana-Champaign

J. C. Chato
University of Illinois at Urbana-Champaign

R6-3

PRESSURE DROP AND HEAT TRANSFER OF MICROFINNED MICROCHANNELS

Christopher A. Monroe, Ty A. Newell*, John C. Chato
monroe1@uiuc.edu, t-newell@uiuc.edu, j-chato@uiuc.edu
Air Conditioning and Refrigeration Center
Department of Mechanical and Industrial Engineering
University of Illinois, 1206 West Green Street, Urbana, IL 61801
*(Tel: 217/333-1655, Fax: 217/333-1942)

ABSTRACT

The primary goal of this project is to characterize the pressure drop and heat transfer of internally enhanced aluminum microchannel tubes in evaporation. Heat transfer and pressure drop tests are being conducted on a smooth walled 6-port microchannel test section and an enhanced test section with hydraulic diameters of 1.69 mm and 0.77 mm, respectively. Test results for R134a with mass fluxes from 100 to 300 kg/m^2-s, at a saturation temperature of 5 C are presented. The results are compared to models to help characterize the effects of the internal enhancements.

INTRODUCTION

Internal surface enhancements have been used extensively in copper tubes to increase their heat transfer capabilities. Aluminum microchannel heat exchangers offer advantages in reduced refrigerant charge and better air side heat transfer when compared to conventional fin-and-tube heat exchangers. The motivation exists to determine if these two effects can be combined to give a better-performing aluminum microchannel.

Typical internal enhancements for copper tubes are on the order of 0.2 mm in depth. Microchannels have been produced with larger scale internal enhancements in which the cross section took on an "H" profile. The surface enhancements used in this project were made on a smaller scale—roughly 0.18 mm in width and 0.38 mm in depth with 12 grooves per port. A picture of the enhanced test section is shown in Figure 1.

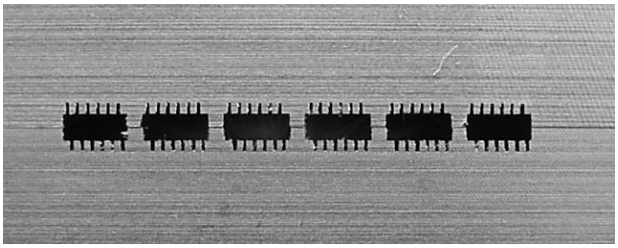

Figure 1: Cross Sectional View of Enhanced Test Section

The enhanced test section was designed as a derivative of the basic test section. In order to keep the cross sections of the two channels similar, the midpoint of the grooves in the enhanced test section is the same as the port depth in the basic test section. After analyzing both sections under a high-power microscope, the actual dimensions resulted in cross sectional areas

that were within 0.1% of each other. This created an interesting result in that when testing at any given mass flux, the corresponding mass flow rate is the same for the two test sections.

EXPERIMENTAL SETUP

The basic and enhanced test sections have been designed and manufactured using CAD/CAM and a CNC mill to ensure accurate dimensions. Each test section consists of two symmetric halves that are bolted together. Figure 2 shows a CAD drawing of the entrance/exit regions of the basic test section. Each half of the test sections is made from a 7.6 x. 53.3 x 0.95 cm (3 x 21 x 3/8") bar of 2024-T6 aluminum. This figure shows the refrigerant entrance/exit hole as well as the pressure tap hole located just outside of the microchannel grooves. A thermocouple is inserted in each entrance/exit hole to give local measurement of the refrigerant temperatures. The seal groove is also visible, going around the circumference of the microchannel grooves but inside of the bolt holes. Each test section half contains four holes drilled in the side, going just below the midpoint of the microchannel grooves. These holes allow the insertion of thermocouple probes in order to get wall temperatures for the heat transfer experiments.

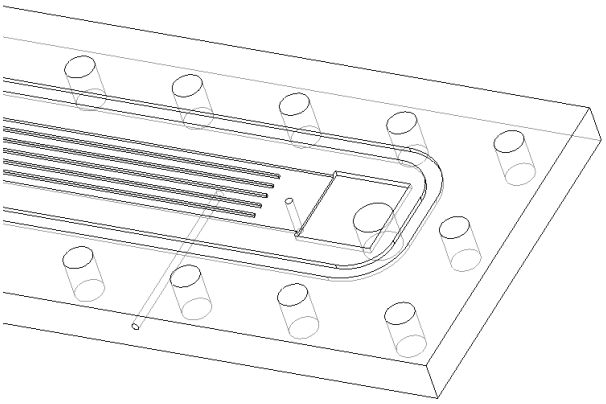

Figure 2: Basic Test Section

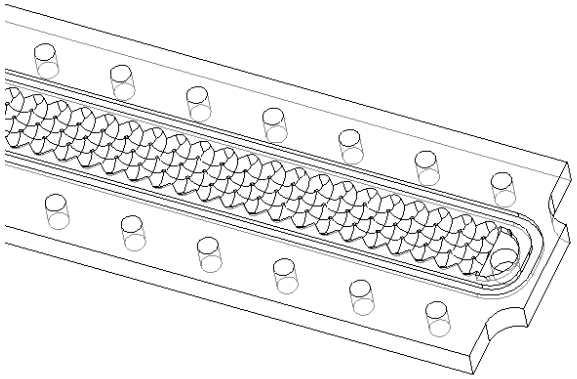

Figure 3: Water Jacket

In order to heat the test sections for the heat transfer experiments, two water jackets are bolted to each side of the microchannel plates. Figure 3 shows a CAD drawing of the end of one of the water jackets. The water jacket plates were designed so that the inlet of the water is directly above the beginning of the microchannel grooves. A chevron surface was used for the water passage in order to increase the turbulence and mixing of the water flow.

Heating water is supplied by a constant temperature bath operating at 9 or 10 C, depending on the test conditions. Water rotameters are used to ensure equal flow between each of the two water jackets per test section. The water flow rate is measured by a turbine flow meter (0-5 L/min, ±2% accuracy) and the inlet and exit temperatures are measured with type-T thermocouple probes. All thermocouple probes were calibrated over their respective ranges of measurement against a NIST traceable precision RTD thermometer (±0.035 C accuracy).

Liquid refrigerant is circulated through the loop using a gear pump located downstream of the receiving tank. The liquid then flows through a coriolis-type mass flow meter (±0.2%

accuracy). Depending on the testing conditions, vapor can be generated using a preheater in the liquid line or directly injected into the system by a vapor compressor. The preheater power input is measured by a power transducer (±0.2% accuracy). The vapor enters the compressor from the top of the receiving tank and its flow is also measured by a coriolis-type mass flow meter (±0.5% accuracy). System temperatures are measured with type-T thermocouples calibrated as described above. The two-phase mixture then flows through the test section, where it is heated by the water jackets. Test section pressure drop is read by a differential pressure transducer (±0.25% accuracy). After leaving the test section, the refrigerant flows through a condenser in order to remove the heat added in the preheater and test section. The refrigerant then returns to the receiving tank.

EXPERIMENTAL PROCEDURE

Tests are conducted over a range of mass fluxes and inlet qualities. The mass fluxes included in the test matrix are 100, 200, and 300 kg/m^2-s, with inlet qualities varying from 0 to 100% in 20% increments. The saturation temperature is 5 C. For heat transfer experiments, the test section heat transfer rate is set according to the following table:

Table 1: Mass Flux, Test Section Heat Transfer Rates, and Corresponding Quality Changes

G (kg/m^{2}s)	Q_{TS} (W)	Δx (%)
100	100	29
200	100	15
300	150	15

The test section heat transfer rates were chosen to keep the quality change low enough so that the refrigerant flow would not drastically change flow patterns, thus affecting the heat transfer coefficients. The decision to compare the results by keeping the total heat transfer rate equal between the two test sections, instead of constant heat flux, was made so that the corresponding quality changes were equal. Having equal quality changes at each data point aids in comparing the pressure drop data.

RESULTS

Figures 4 and 5 show the heat transfer coefficients for the basic and enhanced test sections, respectively, plotted against quality. The individual point on the figures represent the average quality of the refrigerant as it is heated in the test section, with the horizontal bars extending to the entrance and exit qualities. Several trends are observed in the data. First of all, the heat transfer coefficients generally increase as the quality is increased. At lower mass fluxes, this increase is nearly linear, but at higher mass fluxes, the increase begins to exhibit a quadratic form. However, several points do not follow the same general trends. For the four 80% inlet quality points in this data set, the heat transfer coefficient dropped off or did not follow the same increasing trends observed at lower qualities. A possible explanation for this result lies in the liquid layer becoming thinner and less turbulent at higher qualities. When this transition occurs, the liquid layer begins to be dominated by conduction through its thickness rather than convection from its turbulent motion. In addition, the 5% inlet quality point at a mass flux of 100 kg/m^2-s in the basic test section gave a higher heat transfer coefficient than the next higher

quality. Although there is not yet enough data to verify this result, it could be attributable to a higher nucleate boiling contribution in the relatively low-turbulent flow pattern.

Figure 6 shows the enhancement factors defined to compare the two test sections. The data points in this figure represent the average quality, and the horizontal bars are not shown. Two enhancement factors are used for this comparison and are given by the following equations:

$$EF1 = \frac{h_{Enhanced}}{h_{Basic}} \qquad EF2 = \frac{(hA)_{Enhanced}}{(hA)_{Basic}} \qquad (1, 2)$$

The first enhancement factor (EF1) is a direct ratio of the heat transfer coefficients and increases until about 60% quality then begins to decrease. The EF1 values have a minimum value of 1.25 and a maximum value of 2.7, with an average of 1.97. Consequentially, the ratio of the total heat transfer areas of the two test sections is 2.05. Because the EF1 is greater than unity, the results show that even though the enhanced test section has a larger heat transfer surface area, the heat transfer coefficient is also improved.

The second enhancement factor (EF2) includes the ratio of heat transfer areas for the two test sections. Since this ratio is a constant, the EF2 data follow the same trends as for EF1, but are scaled by a constant. The EF2 results show that the extra heat transfer area is being used effectively to give not only an increase of the heat transfer coefficient, but also give an average of four times the heat transfer when compared to the basic test section.

Figure 7 provides the pressure drop gradient data for the two test sections as a function of average quality. Overall, the pressure gradients show a linear increase as the quality is increased. As expected, the pressure gradient increases with mass flux. However, the highest quality data points at a mass flux of 200 kg/m^2-s both appear to drop below this linear relationship. This trend was also observed in previous adiabatic data taken for the basic test section. This result is a product of the liquid layer described above. Since the layer is thinner, and smoother than it is at lower qualities, it does not restrict the flow proportionately more than at lower qualities.

A penalty factor was defined for comparison of the pressure gradients between the two test sections. Figure 8 shows the penalty factor plotted against average quality. The penalty factor is given by the following equation:

$$PF = \frac{(dP/dz)_{Enhanced}}{(dP/dz)_{Basic}} \qquad (3)$$

The penalty factor shows several interesting trends. Having an average value of 2.1, it appears to scale with the hydraulic diameter ratio ($D_{h,basic}/D_{h,enhanced}$), which is 2.2 for these test sections. The penalty factor follows the same, but opposite trend as shown in the pressure gradient data in that it linearly decreases until 60-70% quality then begins to curve up and possibly increase. Furthermore, the penalty factor decreases as mass flux is increased. This result, coupled with increasing heat transfer capabilities at higher mass fluxes, means that the enhanced test section becomes more viable at these conditions.

Work has been done to compare the experimental data to heat transfer and pressure drop correlations found in the literature. Figure 9 shows a comparison of the experimental heat transfer coefficient data to the Wattelet (1994) correlation. The Wattelet correlation is based on data obtained from single-tube evaporation experiments in 7.0 and 10.9 mm diameter copper tubes using R-12, R-22, R-134a, and a 60%/40% azeotropic mixture of R-32/R-125. Wattelet found that the nucleate boiling contribution was dependent on the heat flux and remained prominent at higher qualities and lower heat fluxes. For annular flow patterns and low heat flux, the convective boiling contribution was found to dominate the heat transfer. Figure 9 shows that the Wattelet correlation predicts the heat transfer coefficients for the basic test section to a reasonable degree. However, the correlation severely underpredicts the heat transfer coefficients in the enhanced test section. In general, the Wattelet correlation works better at average qualities below 60%.

Several pressure drop correlations were found in the literature. Figure 10 compares two correlations that showed the best agreement to the experimental data: Zhang and Kwon (1999) and Jung and Radermacher (1989). The Zhang and Kwon correlation is based on adiabatic tests of R-134a, R-22, and R-404a in copper tubes of 6.20 and 3.25 mm diameter and a 6-port aluminum microchannel with hydraulic diameter of 2.13 mm. The Jung and Radermacher correlation is based on flow boiling experiments on pure and mixed R-22, R-114, R-12, and R-152a refrigerants in 9.1 mm diameter stainless steel tubes. Although the Jung and Radermacher correlation was developed for channels much larger than used for this study, it predicted the current heat transfer data and previous adiabatic data in the basic test section quite well. The Zhang and Kwon correlation also gave reasonable prediction of the pressure drop in the basic test section. However, neither of these two correlations, or any others studied, gave acceptable prediction of the pressure drop in the enhanced test section. Further work is in progress to understand the causes of this consistent overprediction for the enhanced test section. Areas to be studied include using the free area (area above the microgrooves) to calculate hydraulic diameter and mass flux for use in the correlations.

CONCLUSIONS

Experimental results show that the enhanced microchannel test section gives a definite improvement in heat transfer coefficient and an overall improvement of roughly four times in the heat transfer capability. As expected, the pressure gradients are higher for the enhanced test section, but show reduced penalty factors for higher mass fluxes and average qualities. Correlations found in the literature predict both pressure drop and heat transfer coefficients well for the basic test section. However, no correlations have been found that adequately predict pressure drop or heat transfer in the enhanced test section.

REFERENCES

Jung, D.S. and Radermacher, R., "Prediction of Pressure Drop During Horizontal Annular Flow Boiling of Pure and Mixed Refrigerants" International Journal of Heat Transfer, Vol. 32, No. 12, pp. 2435-2446, 1989.

Zhang, M. and Kwon, S.L., "Two-Phase Frictional Pressure Drop for Refrigerants in Small Diameter Tubes" Compact Heat Exchangers and Enhancement Technology for the Process Industries, Edited by R.K. Shah, Begell House, New York, 1999.

Wattelet, J.P. and Chato, J.C., "Heat Transfer Flow Regimes of Refrigerants in a Horizontal-Tube Evaporator" ACRC TR-55, Air Conditioning and Refrigeration Center, University of Illinois at Urbana-Champaign, 1994.

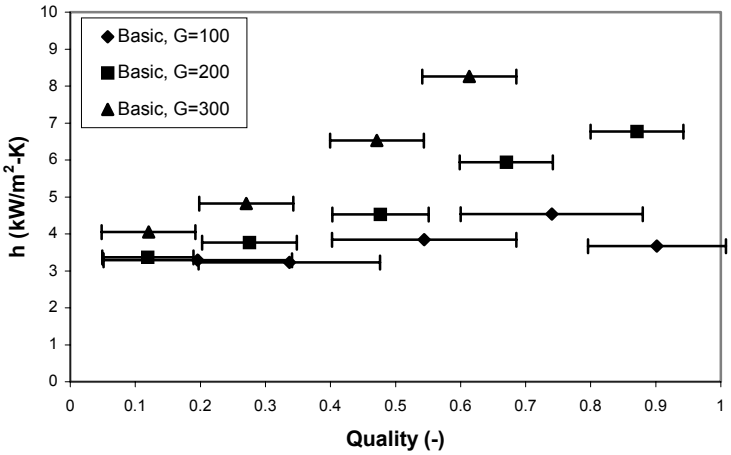

Figure 4: Basic Test Section Heat Transfer Coefficients (Mass Flux, G in kg/m^{2}s)

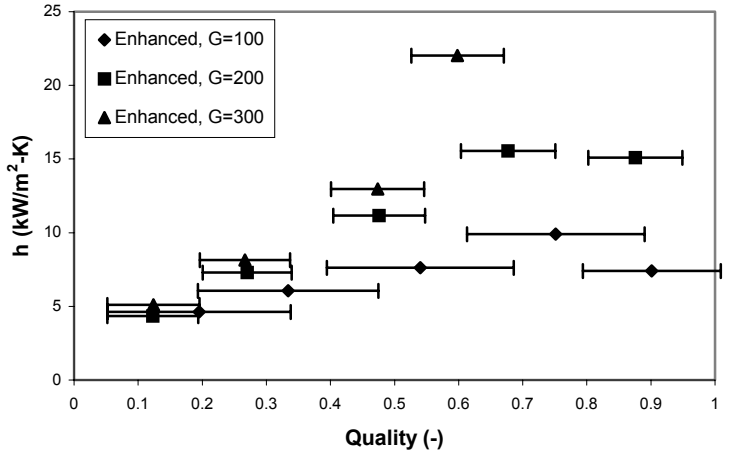

Figure 5: Enhanced Test Section Heat Transfer Coefficients (Mass Flux, G in kg/m^{2}s)

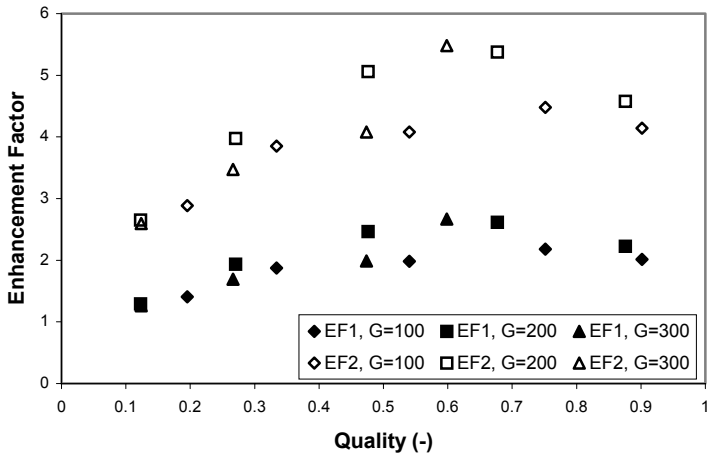

Figure 6: Enhancement Factors for Basic and Enhanced Test Sections (Mass Flux, G in kg/m^{2}s)

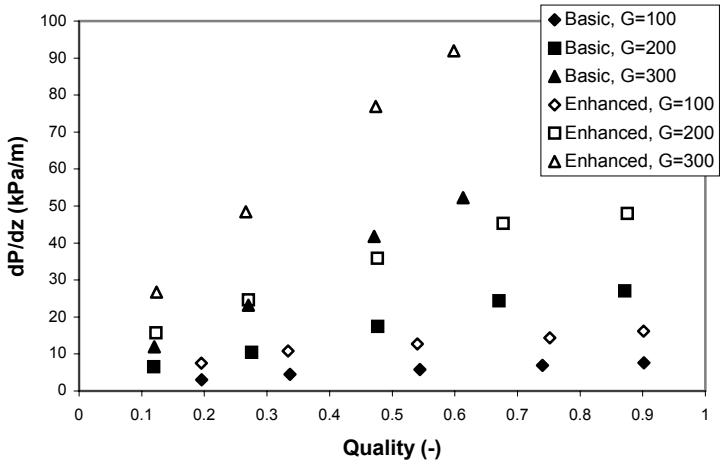

Figure 7: Pressure Drop Data for Basic and Enhanced Test Sections (Mass Flux, G in kg/m^{2}s)

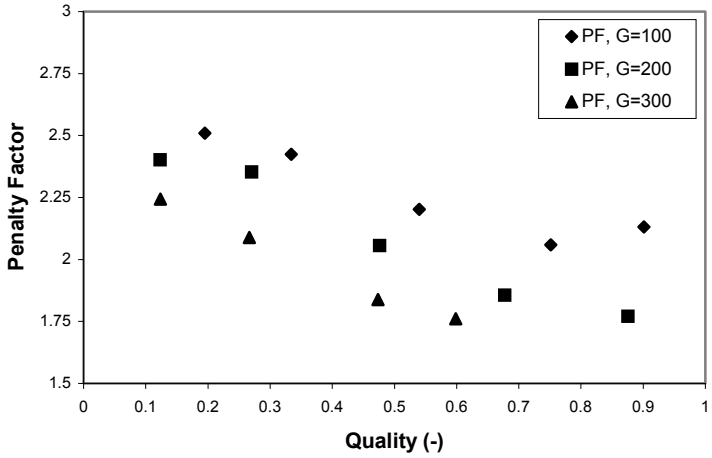

Figure 8: Penalty Factors for Basic and Enhanced Test Sections (Mass Flux, G in kg/m^{2}s)

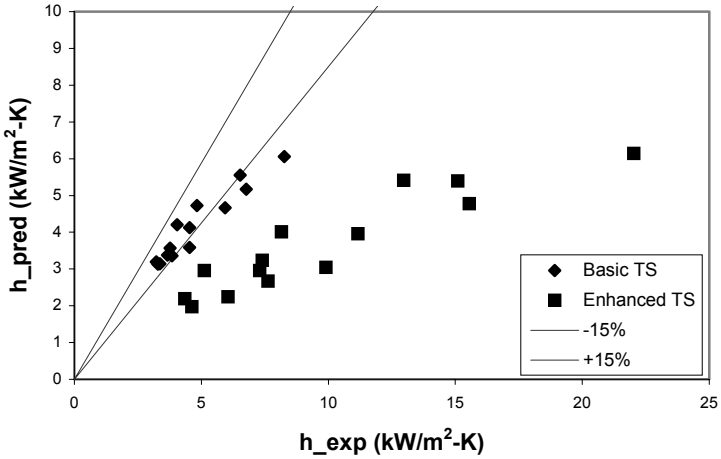

Figure 9: Comparison of Wattelet (1994) Heat Transfer Correlation with Experimental Results

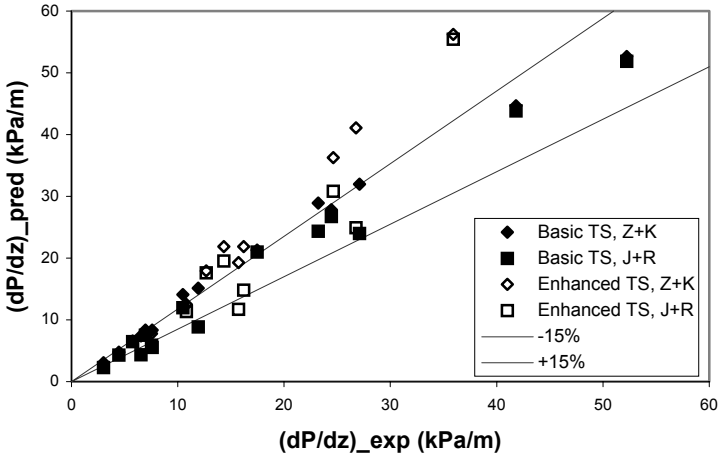

Figure 10: Comparison of Zhang and Kwon (1999) and Jung and Radermacher (1989) Pressure Drop Correlations with Experimental Results